



Anisotropic thermal properties of talc under high temperature and pressure

Akira Yoneda^{a,*}, Mitsuhide Yonehara^a, Masahiro Osako^b

^a Institute for Study of the Earth's Interior, Okayama University, Misasa, Tottori 682-0193, Japan

^b Division of Physical Sciences, National Museum of Nature and Science, Tsukuba, Ibaraki 305-0005, Japan

ARTICLE INFO

Article history:

Received 18 August 2011

Received in revised form 6 October 2011

Accepted 14 October 2011

Available online 31 October 2011

Edited by: Kei Hirose

Keywords:

Talc

Antigorite

Hydrous mineral

Phyllosilicate

Thermal conductivity

Thermal diffusivity

Heat capacity

ABSTRACT

The anisotropic thermal conductivity and diffusivity of talc were simultaneously measured up to 5.3 GPa and 900 K using the pulse transient method. Although significant anisotropy was observed in the thermal conductivity of talc, the average thermal conductivity is comparable to that of olivine and roughly three times greater than that of antigorite. From the ratio of the thermal conductivity to the thermal diffusivity, the heat capacity of talc was evaluated. The pressure derivative of heat capacity was found to be positive, which is related to the anomaly of thermal expansivity of talc above 50 °C at atmospheric pressure.

© 2011 Elsevier B.V. All rights reserved.

1. Introduction

Talc, $\text{Mg}_3\text{Si}_4\text{O}_{10}(\text{OH})_2$, is a major hydrous metamorphic mineral. It is a phyllosilicate, or sheet silicate mineral, with a monoclinic crystal symmetry (Fig. 1). It is well known as the softest mineral, with a rating of 1 on Moh's scale of hardness. Owing to its unique mechanical and chemical qualities, it has been frequently used as an industrial material, such as a lubricant, a filler, and a pressure-transmission material in high-pressure experiments.

Talc is expected to exist in subducting slabs. Recently, the dehydration of talc has been implicated as a possible earthquake trigger in the shallower parts of a subducting slab (e.g., Omori et al., 2004). Since slab dehydration is partially controlled by the temperature in the slab, the thermal conductivity of talc is an important factor for controlling the temperature distribution, the dehydration sequence, and thus slab seismicity.

Anisotropy is a common physical property of sheet structure materials like talc. To examine anisotropic thermal conductivity in natural talc, or more generally a polycrystalline aggregate with preferred orientation, we selected natural talc with a dominant foliation for experimentation. The pulse transient method enables us to examine anisotropic thermal conduction in such a sample.

The other advantage of the pulse transient method is that we can determine the heat capacity from thermal diffusivity, κ , and

thermal conductivity, λ , using the relationship $\lambda = \rho C \kappa$, where ρ is density and C is heat capacity.

2. Experiment

The specimens analyzed here were produced from a natural talc block produced in Guangxi, China. It is slightly greenish with pronounced foliation. Through powder X-ray diffraction, the sample was identified as single phase of pure talc with monoclinic symmetry (Stemple and Brindley, 1960). Its nominal density was 2716 kg/m³, which is 2.4% less than talc's X-ray density of 2783 kg/m³. The stoichiometry was confirmed as $(\text{Mg}_{0.99}\text{Fe}_{0.01})_3\text{Si}_4\text{O}_{10}(\text{OH})_2$ by means of electron microprobe analysis.

We designated the Z direction as the direction normal to the foliation plane. Then, we specified the other two directions based on ultrasonic velocity measurements. The X and Y directions are set to be the faster and the slower polarized directions, respectively, of shear waves propagating in the Z direction. Table 1 summarizes the acoustic velocity measurements of the talc sample at ambient conditions. The arithmetically averaged P - and S -wave velocities (V_p and V_s) are 4.70 km/s and 2.06 km/s, respectively. Bailey and Holloway (2000) reported that V_p for sintered talc is 5.27 km/s at 0.5 GPa. The ~11% difference may be attributed to an intrinsic pressure effect, porosity collapse, or anisotropy in the sintered sample.

Fig. 2 shows a photograph of the talc and its microscopic texture in the Y direction. We can observe a pronounced foliation and lineation structure, oriented in the Z and X directions, respectively. The talc rock sample is the same one that Guo et al. (2011) used

* Corresponding author. Tel.: +81 858 43 3762; fax: +81 858 43 2184.

E-mail address: yoneda@misasa.okayama-u.ac.jp (A. Yoneda).

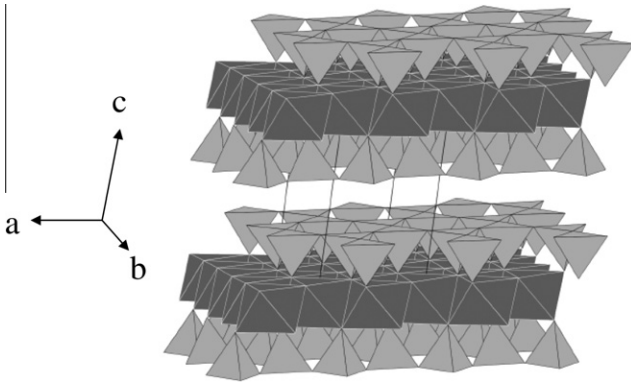


Fig. 1. Crystal structure of talc. It is composed of layers of tetrahedron and octahedron sheets. Si and Mg atoms are inside the tetrahedrons and octahedrons, respectively.

Table 1
Acoustic wave velocities of talc in km/s. Diagonal components are P wave velocity, and off-diagonal ones are S wave velocity.

		Propagating direction		
		X	Y	Z
Polarized direction	X	5.78	2.71	1.87
	Y	2.69	4.52	1.63
	Z	1.83	1.65	3.80

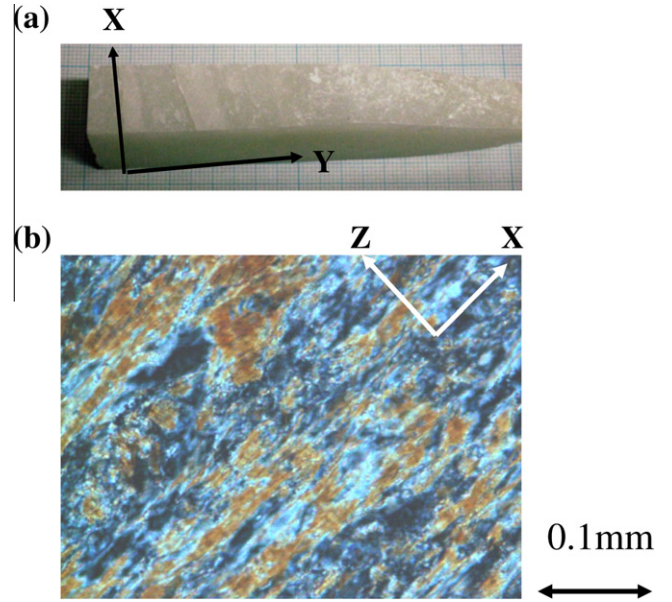


Fig. 2. (a) Photograph of a block used in the present work. The X and Y directions are specified by arrows. The Z direction is normal to the foliation surface. (b) Polarized microscope view on a thin section in the Y direction. X and Z directions are specified by white arrows. Note the relatively fine grain texture.

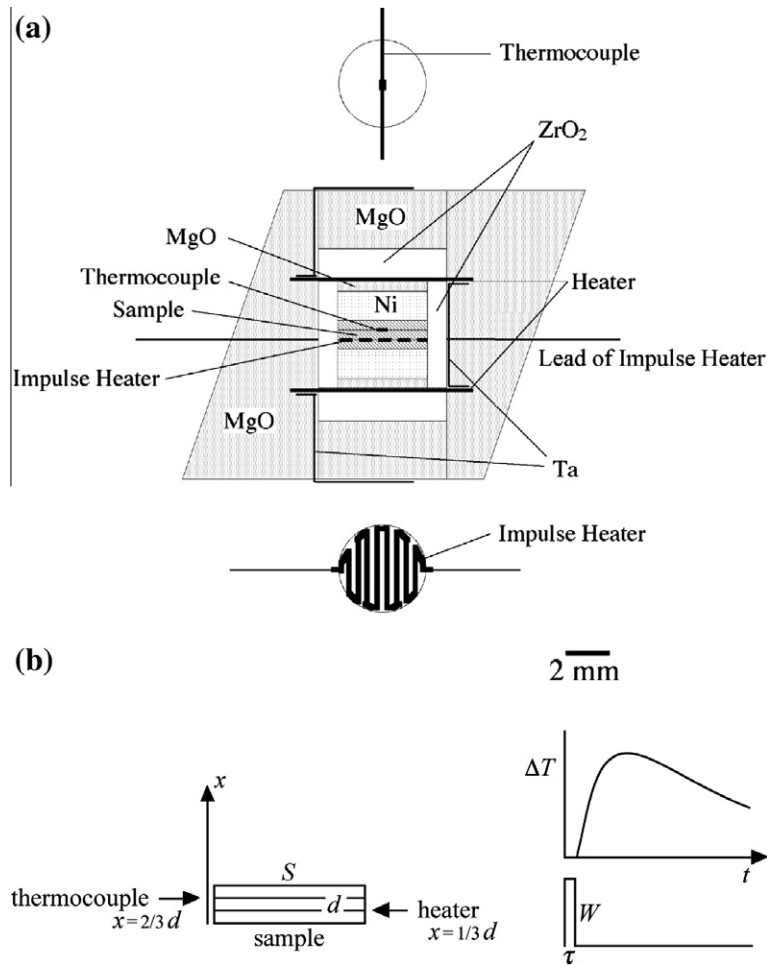


Fig. 3. (a) Cross section of the sample assembly for the pulse transient method (Osako et al., 2004). (b) Concept of the pulse transient method. Left figure shows basic configuration of the sample. d is the total height of the three sample disks, S is the area of the heater, x is the position from the bottom of the sample (the heater is at $x = d/3$, and the thermocouple is at $x = 2d/3$). Temperature change ΔT caused by impulse heating with a power of W is monitored by the thermocouple (right figure), where τ is the duration of pulse heating, and t is time from onset of the heating.

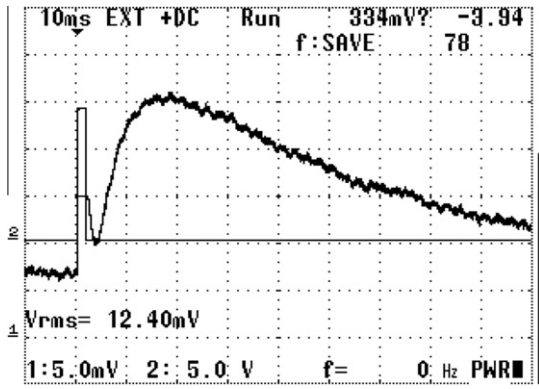


Fig. 4. An example of the oscilloscope display in the present study. Channels 1 and 2 were used to monitor thermocouple output and voltage for impulse heater (see Fig. 1b), respectively. Note that the Channel 1 data were magnified 1000 times by a DC amplifier. The corresponding digitized data of Channel 1 were used for curve fitting to determine parameters A and B in Eq. (2).

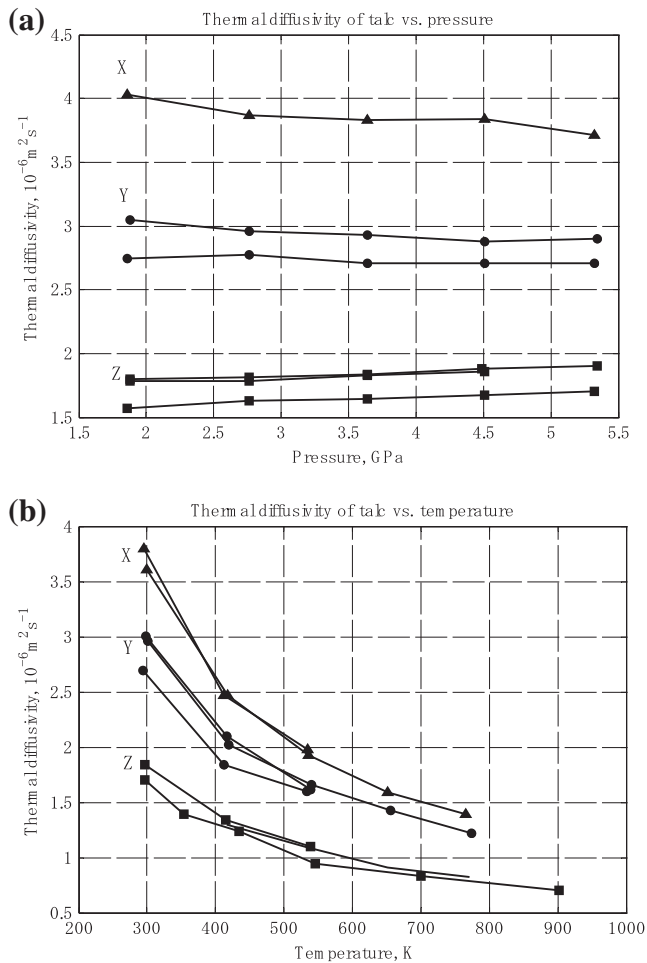


Fig. 5. Thermal diffusivity results. (a) Pressure dependence. (b) Temperature dependence at 5.3 GPa. The temperature dependence was measured during temperature decreasing process in multiple heating. Triangle (\blacktriangle), circle (\bullet), and square (\blacksquare) symbols correspond to X, Y, and Z directions, respectively, of the present talc block.

in their electrical conductivity measurements. They confirmed that the {001} plane series is concentrated in the Z direction specimen.

We prepared disks (4.3 mm in diameter and ~ 0.33 mm thick) of talc oriented in three directions for measurements under high

pressure and high temperature. Fig. 3 shows the cell assembly and the concept of the present pulse transient method. The details of the experimental procedures were reported previously (Osako et al., 2004).

In the high pressure and temperature measurements, we first measured the pressure dependence of thermal properties up to 5.3 GPa at room temperature, and then heated it to a higher temperature at 5.3 GPa. We checked mineral phase of recovered talc sample, because the extrapolation of the phase boundary suggests decomposition of talc at around 900 K at 5.3 GPa (Bose and Ganguly, 1995). X-ray analysis confirmed that no phase change for talc sample recovered from 670 K heating, and trace of decomposition for the one from 900 K heating. Thus we can conclude that the present experiment data corresponds to pure talc.

Fig. 4 shows an example of the thermal pulse observed in the present work. The acquired data were analyzed based on an explicit equation solved under the assumption of one-dimensional heat flow and constant temperature boundary conditions (Dzhavadov, 1975):

$$\Delta T = A \sum_{n=1}^{\infty} \frac{1}{n^2} \sin \frac{n\pi}{3} \sin \frac{n\pi x}{d} \exp(-n^2 B t) [\exp(n^2 B \tau) - 1] : (t > \tau) \quad (1)$$

where t is the time from the onset of heating, x is the position measured from the end of the sample, d is the total height of the three sample disks, and τ is the duration of the heating pulse. The quantities A and B are defined as

$$A = \frac{2Wd}{\pi^2 \lambda S}, \quad B = \frac{\pi^2 k}{d^2} \quad (2)$$

where W is the power of the impulse heating and S is the area of the heater. The pressure and temperature effects on d and S were corrected based on Gleason et al. (2008) and Pawley et al. (1995).

3. Results and discussion

Fig. 5 shows the results of the talc thermal diffusivity investigation. Note that measurements were conducted once, twice, and three times, in the X, Y, and Z directions. The reproducibility was within $\sim 15\%$ in the Z direction. These results show a pronounced anisotropy in the thermal properties. As in the cases of acoustic velocity and electrical conductivity, the magnitude of thermal diffusivity is also observed to have a strong directional dependence (Guo et al., 2011). The pressure derivatives of thermal diffusivity are negative, nearly zero, and positive in the X, Y, and Z directions, respectively. This may be an intrinsic behavior of anisotropic thermal diffusivity in talc. An alternative interpretation is that it is due to rotation of the sheet layer in talc during compression. Regardless of the mechanism, we can conclude that average thermal diffusivity of talc is nearly constant at around $\sim 2.8 \times 10^{-6} \text{ m}^2/\text{s}$ over the present pressure range. As for the temperature dependence of thermal diffusivity, the decrease is commonly as large as 60% in every direction between 300 and 900 K.

Fig. 6 shows the thermal conductivity measured here in comparison with other materials. The experimental scatter in the Y and Z directions is $\sim 20\%$, approximately twice of that of thermal diffusivity. As shown in Eq. (2), thermal conductivity is related to W/S (heat generation per area), which may be an additional source of error when compared with the thermal diffusivity measurements made here. In spite of the scatter, we can see that the average thermal conductivity is $\sim 7 \text{ W m}^{-1} \text{ K}^{-1}$, with only a small pressure dependence. As for the temperature dependence of thermal conductivity, we recognize a common decrease of $\sim 40\%$ in every direction between 300 and 900 K. Note that both the thermal diffusivity and the thermal conductivity of talc show a decrease

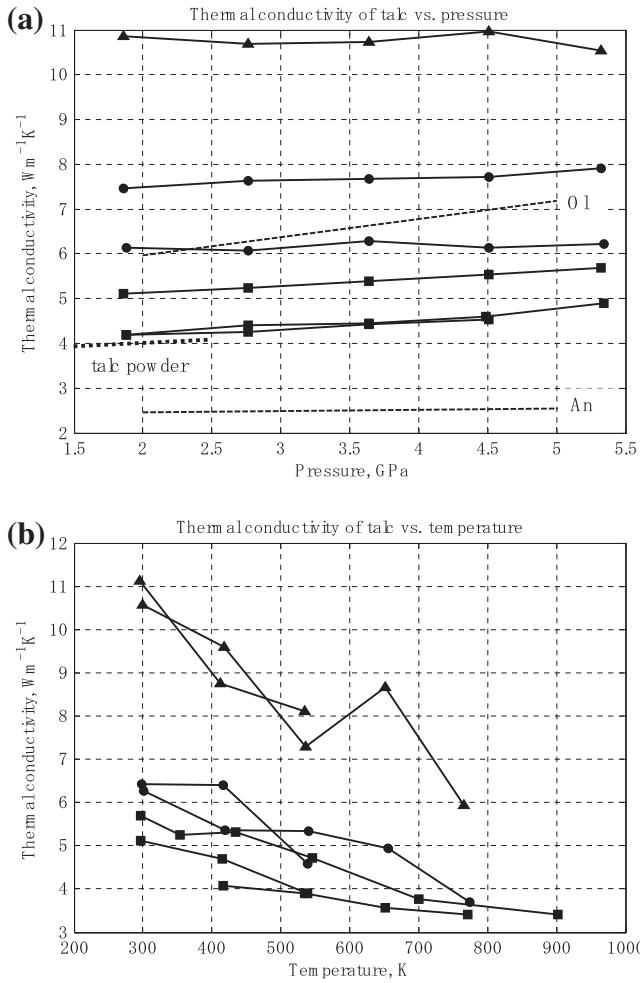


Fig. 6. Thermal conductivity results. (a) Pressure dependence. The dotted line is the data for sintered talc from powder (Gummow and Sigalas, 1988). The dashed lines are olivine (OI; Osako et al., 2004) and antigorite (An; Osako et al., 2010) data, as references. (b) Temperature dependence at 5.3 GPa. Triangle (\blacktriangle), circle (\bullet), and square (\blacksquare) symbols correspond to X, Y, and Z directions, respectively, of the present talc block.

similar to that seen in olivine and garnet, and a much larger decrease than that of antigorite.

Earlier data collected by Gummow and Sigalas (1988) were similar to the lower bounds of the Z-oriented conductivity measured here. This suggests that the compacted powder sample may cause a significant preferred orientation of the *c* axis. On the other hand, Horai (1971) reported $7.0 \text{ W m}^{-1} \text{ K}^{-1}$ for the thermal conductivity of talc at ambient conditions. His specimen, a mixture of powdered mineral and distilled water, seemed to be isotropic, compared with the present result.

It is surprising that the thermal conductivity of talc is comparable to that of olivine and as much as three times higher than that of antigorite, although V_p of antigorite ($\sim 6.7 \text{ km/s}$) is faster than that of talc in any direction (Table 1). This apparent contradiction may be attributable to antigorite's alternating wavy structure at a wavelength of a few nanometers (e.g., Watanabe et al., 2007). In contrast with antigorite, the sheet layering of talc is smooth enough to propagate acoustic waves and phonons. This suggests that the sheet layer characteristics in a phyllosilicate can control macroscopic physical properties.

Fig. 7 shows the results of the talc heat capacity investigation. Although the results are scattered by as much as $\pm 20\%$, the average is $\sim 1000 \text{ J kg}^{-1} \text{ K}^{-1}$ at around 3.5 GPa. The extrapolated value at

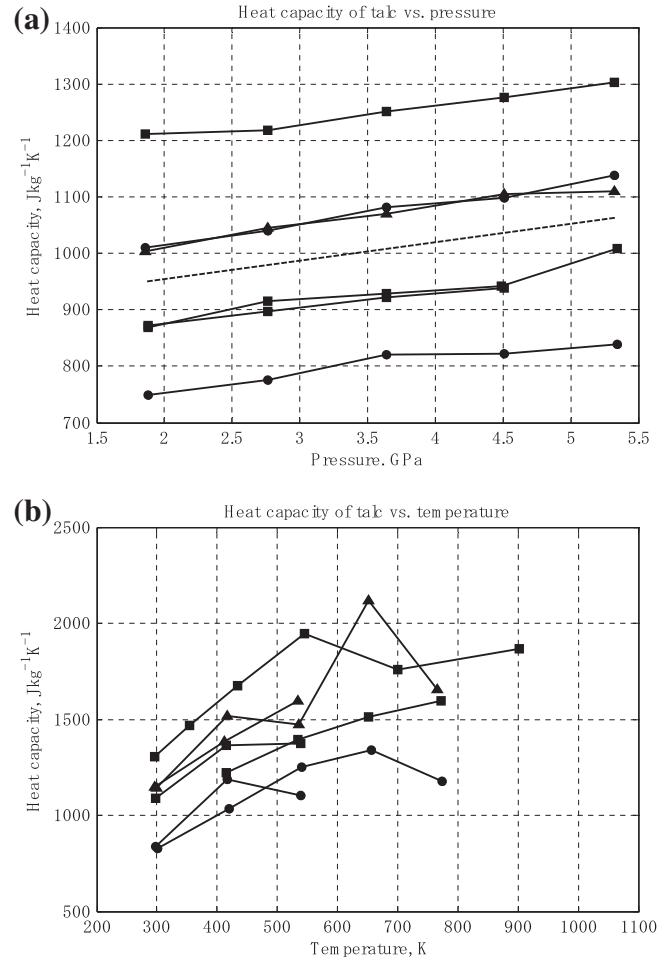


Fig. 7. Heat capacity results. (a) Pressure dependence. The dashed line is the average of the six measurements. (b) Temperature dependence at 5.3 GPa. Triangle (\blacktriangle), circle (\bullet), and square (\blacksquare) symbols correspond to X, Y, and Z directions, respectively, of the present talc block.

atmospheric pressure is $\sim 890 \text{ J kg}^{-1} \text{ K}^{-1}$, which is close to the reported value of $852 \text{ J kg}^{-1} \text{ K}^{-1}$ for the heat capacity of talc at atmospheric pressure (Robie and Stout, 1963; Hemingway, 1991). Note that the heat capacity of talc is comparable to that of antigorite (Osako et al., 2010). We can see that the heat capacity of hydrous minerals exceeds that of non-hydrous minerals, such as olivine and garnet, by $\sim 30\%$ (Watanabe, 1982; Osako et al., 2004). Therefore, it is reasonable that hydrous minerals could have more vibrational freedom because of the presence of the lightest element, hydrogen, in the crystal structure. As for the temperature dependence of heat capacity, we recognize an increasing trend of heat capacity with temperature; however, the quality may not be enough for further scientific implication.

In spite of the scatter of the absolute value of heat capacity itself, their slopes against pressure are quite consistent with each other, yielding

$$\left(\frac{\partial C_p}{\partial P}\right)_T \approx 28 \text{ J kg}^{-1} \text{ K}^{-1} \text{ GPa}^{-1} \approx 2.8 \times 10^{-8} \text{ m}^3 \text{ kg}^{-1} \text{ K}^{-1} \quad (3)$$

This value was used previously (Osako et al., 2010) to explain an anomalous thermal expansion reported by Pawley et al. (1995).

4. Conclusion

The anisotropy of thermal diffusivity and thermal conductivity in talc has been measured at high pressure and temperature. Large

anisotropy is confirmed, as expected, for phyllosilicate sheet minerals. However, the thermal conductivity of talc was found to be comparable to that of olivine. This finding was not imagined prior to the analysis presented here. Although both talc and antigorite are common soft hydrous minerals with low mechanical strength, the thermal properties of talc are more similar to rock forming minerals like olivine, than they are to those of antigorite. As a result, talc does not assume a special role in the subducting slab from the viewpoint of heat and temperature phenomena, i.e., talc cannot be implicated in the formation of a thermal boundary layer in the subducting slab.

Acknowledgements

This work was supported by a Grants in Aid for Scientific Research (Nos. 19204044 and 21540444) from the Ministry of Education, Culture, Sports, Science and Technology, and was carried out by joint research at the Institute for Study of the Earth's Interior, Okayama University. The authors thank S. Maruyama, N. Tomioka and T. Tsujimori for characterizing the present sample, and T. Maeda and C. Oka for assistance with the high-pressure experiment.

References

- Bailey, E., Holloway, J., 2000. Experimental determination of elastic properties of talc to 800 °C, 0.5 GPa; calculation of the effect on hydrated peridotite, and implications for cold subduction zones. *Earth Planet. Sci. Lett.* 183, 487–498.
- Bose, K., Ganguly, J., 1995. Experimental and theoretical studies of the stabilities of talc, antigorite and phase A at high pressures with applications to subduction processes. *Earth Planet. Sci. Lett.* 136, 109–121.
- Dzhavadov, L.N., 1975. Measurement of thermophysical properties of dielectrics under pressure. *High Temp.-High Pressures* 7, 49–54.
- Gleason, A.E., Parry, S.A., Pawley, A.R., Jeanloz, R., Clark, S.M., 2008. Pressure-temperature studies of talc plus water using X-ray diffraction. *Am. Mineral.* 93, 1043–1050.
- Gummow, R., Sigalas, I., 1988. The thermal conductivity of talc as a function of pressure and temperature. *Int. J. Thermophys.* 9, 1111–1120.
- Hemingway, B.S., 1991. Thermodynamic properties of anthophyllite and talc: Corrections and discussion of calorimetric data. *Am. Mineral.* 76, 1589–1596.
- Guo, X., Yoshino, T., Katayama, I., 2011. Electrical conductivity anisotropy of deformed talc rock and serpentinites at 3 GPa. *Phys. Earth Planet. Int.* 188, 69–81.
- Horai, K., 1971. Thermal conductivity of rock-forming minerals. *J. Geophys. Res.* 76, 1278–1308.
- Omori, S., Komabayashi, T., Maruyama, S., 2004. Dehydration and earthquake in the subducting slabs: empirical link in intermediate and deep seismic zones. *Phys. Earth Planet. Int.* 146, 297–311.
- Osako, M., Ito, E., Yoneda, A., 2004. Simultaneous measurements of thermal conductivity and thermal diffusivity for garnet and olivine under high pressure. *Phys. Earth Planet. Int.* 143–144, 311–320.
- Osako, M., Yoneda, A., Ito, E., 2010. Thermal conductivity, thermal diffusivity, and heat capacity, of serpentine (antigorite) under high pressure. *Phys. Earth Planet. Int.* 183, 229–233.
- Pawley, R.P., Redfern, S.A.T., Wood, B.J., 1995. Thermal expansivities and compressibilities of hydrous phases in the system MgO–SiO₂–H₂O: talc, phase A and 10-Å phase. *Contrib. Mineral Petrol.* 122, 301–307.
- Robie, R.A., Stout, J.W., 1963. Heat capacity from 12 to 350 K and entropy of talc and tremolite. *J. Phys. Chem.* 67, 2252–2256.
- Stemple, I.S., Brindley, G.W., 1960. A structural study of talc and talc-tremolite relations. *J. Am. Ceram. Soc.* 43, 34–42.
- Watanabe, T., Kasami, H., Ohshima, S., 2007. Compressional and shear wave velocities of serpentinized peridotites up to 200 MPa. *Earth Planets Space* 59, 233–244.
- Watanabe, H., 1982. Thermochemical properties of synthetic high-pressure compounds relevant to the Earth's mantle. In: Akimoto, S., Manghnani, M.H. (Eds.), *High Pressure Research in Geophysics*. Center for Academic Publication, Tokyo, pp. 441–464.